Online Trace Detection of Mercury Ions with Enhanced Fluorescence Excitation within Metal-lined Hollow-core Fiber

HAONAN DING[1,2], JIECHEN ZHANG[1,2], XIAOXIAN LIU[1,2], YIFAN ZHU[1,2] ZHENYONG DONG [1,2], DORA JUAN JUAN HU[3], GUANGHUI WANG[1,2]*

[1]College of Engineering and Applied Sciences, Nanjing University, Jiangsu 210093, China
[2]Key Laboratory of Intelligent Optical Sensing and Integration of the Ministry of Education, Nanjing University, Jiangsu 210009, China
[3]Institute for Infocomm Research, Agency for Science, Technology and Research, Singapore 138632, Singapore
*Corresponding author: wangguanghui@nju.edu.cn

Received XX Month XXXX; revised XX Month, XXXX; accepted XX Month XXXX; posted XX Month XXXX (Doc. ID XXXXX); published XX Month XXX

In this letter, we present a portable all-fiber fluorescent detection system based on metal-lined hollow core fiber (MLHCF) for the ultra-sensitive real-time monitoring of mercury ions (Hg^{2+}). The system employs the rhodamine derivative as the probe. The hollow core of the MLHCF serves as both the flow channel of the liquid sample and the waveguide of the optical path. The metal coating in the intermediate layer between the capillary and the polyimide coating in the MLHCF provides good light confinement, enhancing the interaction between the sample and the incident light for better fluorescence excitation and collection efficiency. Additionally, further enhancement is achieved by placing an inserted filter along the light path to reflect the excitation light back to the MLHCF. A 3 cm length of MLHCF enables simultaneous excitation of 40 μL sample volume and collection of most of its fluorescent signal in all directions, thereby significantly contributing to its exceptional sensitivity with a limit of detection of 2.3 ng/L. The all-fiber fluorescence-enhanced detection device also shows rapid response time, excellent reusability, and selectivity. This system presents an online, reproducible and portable solution for the trace detection of Hg^{2+}, and provides a promising way in detecting other heavy metal ions.

http://dx.doi.org/10.1364/OL.99.099999

In recent years, there has been a growing emphasis on water safety, leading to the growing attention towards the detection of heavy metal ions. As a typical heavy metal pollution of water, mercury pollution has been classified as a global pollutant by the United Nations Environment Programme (UNEP) due to its persistent, migratory, highly bioconcentrated and intense nature [1]. Prolonged use of drinking water containing traces of mercury ions will result in cumulative poisoning, which can be extremely damaging to the optic nerve of the brain [2]. Therefore, in past decades, trace detection techniques for mercury ions have attracted the interest of scientists, and a variety of mercury ion detection methods have been developed [3].

Traditional heavy metal detection methods, such as atomic fluorescence spectrometry, coupled plasma-mass spectrometry, and gas chromatography-mass spectrometry, are expensive and require complex pretreatment processes, making them unsuitable for rapid detection [4]. On the other hand, fluorescence probes method could be used for the detection of mercury ions in food safety, pharmacology and materials, which has the advantages of cost-effective, ease of operation and low detection limits [5]. A variety of fluorescent probes are available for the detection of mercury ions, including quantum dot fluorescent probes, ratiometric fluorescent probes and small molecule classes [6]. Considering the requirement of rapid detection, small molecule fluorescent probes such as rhodamine derivatives can react quickly within seconds and have the advantage of simple preparation [7].

In order to enhance the fluorescence signal and collection efficiency, fiber optic sensors have been proposed as a means of carrying out fluorescence detection, which is also applicable for rapid and convenient online monitoring [8]. In 2019, Nguyen et al. designed a method of fixing fluorescent polymeric material to the end face of an optical fiber to increase the corresponding fluorescence intensity of Hg^{2+} through a photoinduced electron transfer mechanism, achieving a detection limit of 0.15 μM (30 μg/L) [9]. However, the interaction between light and material in this way is restricted to the end surfaces of the fiber, with limited enhancement of the fluorescence signal, and could not perform high-precision measurements.

Therefore, special hollow-core fiber (HCF) such as hollow-core photonic crystal fibers (HCPCF) and hollow-core anti-resonant fibers (HCARF) attract attention because the hollow core will provide a flow channel and light path to enhance light-matter interaction [10, 11]. In addition, HCF can be combined with cavity enhancement spectroscopy by placing a reflector on the end face for multiple excitations to improve the detection signal [12]. However, since the inner diameter of HCPCF is only a few tens of microns, requiring high-pressure strength to inject

liquid. Metal-lined hollow-core fiber (MLHCF) with an inner diameter of several hundred microns would be a better choice. This type of fiber enables liquid injection without high pressure. It is suitable for use in fast and simple in-line type detection solutions. Furthermore, the metal layer on its inner wall facilitates total reflection, effectively trapping the incident light inside for multiple excitations, and increasing the collection efficiency of fluorescence, resulting in significant signal enhancement [10]. With the aforementioned advantages, MLHCF is suitable for fast and easy online liquid detection.

In this letter, we developed a compact all-fiber and rapid online system for detecting mercury ions in water utilizing MLHCF combined with rhodamine derivatives as fluorescence probes. Firstly, MLHCF chips were prepared and used to build an all-fiber fluorescence sensing system. The fluorescence detection enhancement effect of MLHCF was validated in this step. Secondly, a rhodamine B hydrazide derivative named SD was synthesized, which specifically bound with mercury ions and emitted fluorescence at 590 nm; Finally, this system was demonstrated to achieve successful detection of mercury ions across a wide range of concentrations, as well as to specifically detect a low concentration of mercury ions.

We firstly characterize the parameters which affect the fluorescence intensity. Under dilute solution conditions, the fluorescence intensity can be approximated by the Taylor expansion as:

$$F = \varphi I_0(1 - 10^{-\varepsilon lc}) = 2.3\varphi I_0 \varepsilon lc, \quad (1)$$

where φ and ε denote the fluorescence quantum yield and molar absorption coefficient, respectively. I_0 is the intensity of incident light. l represents the thickness of the liquid cell. c denotes the concentration of the substance to be measured. According to Eq. 1, we can observe that fluorescence intensity is directly proportional to the concentration of the substance being measured, as well as to the path length and the incident light intensity [12]. The focus in this study is to establish the quantifiable correlation between the concentration of the sample and its fluorescence intensity. This correlation will enable us to obtain quantitative information on the concentration based on the measured fluorescence intensity.

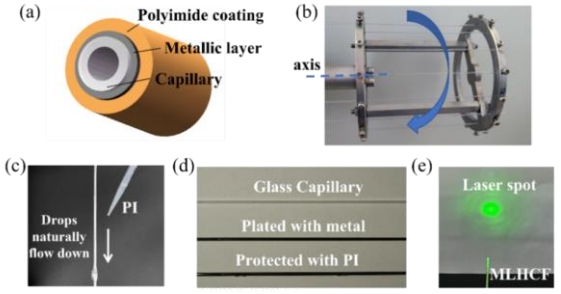

Fig. 1. (a) The internal structure diagram of MLHCF. (b) Capillary rotary coating fixture. (c) PI naturally downwards by gravity and coats evenly on the capillary plated with metal. (d) Hollow core glass capillary without metal coating, capillary after metal plated and MLHCF after protected with PI. (e) The laser spot is emitted by the excitation light after passing through MLHCF.

MLHCF is a special optical fiber, made by coating the walls of a hollow-core glass capillary with metal followed by a polyimide-coated protective layer [13], the internal structure diagram is shown in Fig. 1(a). In this study, we chose to aluminize the outer wall of hollow core fibers, which with an inner diameter of 680 μm and an outer diameter of 1000 μm. Metallic aluminum is capable of reflecting up to 88% of visible light, making it ideal for confining both excitation light and fluorescence in the capillary core. The hollow core structure of MLHCF also enhances the interaction of excitation light with the sample, thereby increasing the signal collection efficiency. In addition, the large inner diameter of the aluminized capillaries, which can reach several hundred microns, provides several advantages such as broad bandwidth, simple preparation methods, and low cost. Another important point is that liquids can be directly injected into the capillaries at atmospheric pressure, making it suitable for fast and easy online detection with minimal cross-contamination during sample exchange.

We chose the high vacuum resistance evaporation coating equipment (VNANO/VZZ-300S, Beijing Wiener Vacuum Technology Co., Ltd) to coat the walls of the hollow-core fiber with a metal film, this method can vapor-deposit the end surface of the part or the outer wall of the glass tube, with the rotary axis fixing the capillary as shown in Fig 1(b). Polyimide (PI) was then diluted with N, N-dimethylformamide (DMF) in a 10:1 ratio to a suitable consistency. Following this, the diluted PI was uniformly applied to the outer surface of the metal films under the influence of gravity, as shown in Fig. 1(c). The PI drops naturally flowed down along the vertically placed capillary. The capillary was rotated while the PI was falling, enabling the formation of a consistent and uniform layer on the surface of the capillary. Next, the capillary tube was baked at 240°C for 50 minutes to form a cured coating on the surface to enhance capillary toughness and protect the metal film from abrasion. In this way, we have prepared MLHCFs with a metal layer thickness of approximately 70 nm. As shown in Fig 1(d), three different states of capillaries before and after metal coating, and after the protection with PI are illustrated. When MLHCF processing has been completed, we examined its light-guiding effect using a 532 nm laser, the outgoing light shown in Fig. 1(e), shows a good laser spot and the enhancement up to 9.4 times compared to the normal capillary without metal plating.

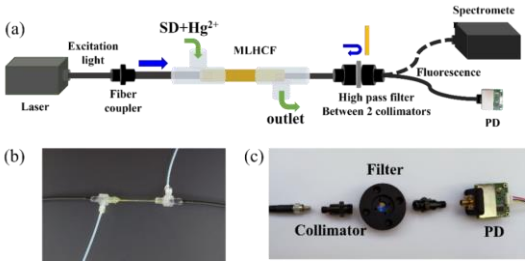

Fig. 2. (a) the internal structure diagram of MLHCF. (b) Package diagram of the MLHCF. (c) Experiment set-up of the all-fiber fluorescence detection device.

For fast and portable detection, an all-fiber fluorescence detection device was developed as shown in Fig. 2(a). An all-fiber fluorescence detection device was developed for fast and portable detection. Firstly, the MLHCF was packaged into a microfluidic chip, and a double three-way valve structure was used to realize the input and output of the sample and the input and output of the optical signal simultaneously, as shown in Fig. 2(b). Following this, a plastic optical fiber was used as the optical transmission fiber, which was coupled to both ends of the MLHCF by insertion. 532 nm laser light entered the input fiber, and an automatic syringe pump was used to inject the sample through the gap between the MLHCF and the input fiber into the hollow core of the MLHCF, where it interacted with the excitation light, and subsequently emitted outputs fluorescence and excitation light through the output

fiber. Notably, since the fluorescence wavelength (about 590 nm) was longer than wavelength of excitation light (532 nm), a long-pass filter with a cut-off wavelength of 550 nm was used to pass the fluorescence while reflecting the excitation light for folded excitation, which further enhanced the fluorescence signal. The parts used for filtering are shown in Fig 2(c). A good filtering effect can be achieved by using two collimators to focus the light and fix the filter.

Finally, as shown in Fig 2(a), a photodetector (PD) or spectrometer was connected at the end of the system to receive the fluorescence signal. The spectrometer can detect the spectrum of fluorescent signals to obtain information such as wave peaks and waveforms, but the sensitivity is insufficient. The PD can only obtain the fluorescence light intensity, but the sensitivity is very low. Therefore, we combined these two detection methods in subsequent experiments.

The chemical reagents used in the experiment such as mercury standard (5 μg/L), Rhodamine B hydrazide ($C_{28}H_{33}ClN_4O_2$), 2-Hydroxy-5-methoxybenzaldehyde ($C_8H_8O_3$), Dimethylformamide (DMF) and Ethanol anhydrous (C_2H_{60}), etc., unless otherwise specified were procured from Nanjing Wanqing chemical glass ware & Instrument Co. Ltd. Sodium standard solution purchased from Beijing North Weiye Institute of Metrology and Technology.

The main operating mode of Rhodamine type probes is similar to that of a switch, which is an (off-on) reversible mode. The probe does not fluoresce when the spiroloop is closed, but fluoresces strongly when the spiroloop is open. When a suitable receptor is modified on the rhodamine spiro ring structure, it can selectively interact with a specific metal ion to open the spiro ring and eventually turn on the fluorescent signal [14]. The fluorescence probe we used here is called 2-Hydroxy-5-methoxybenzaldehyde rhodamine hydrazide (SD). Its synthesis and the complexation interaction with the mercury ion was performed as shown in Fig. 3(a). Briefly, 2-Hydroxy-5-methoxybenzaldehyde (250 mg, 0.5 mmol) and Rhodamine B hydrazide (78 mg, 0.5 mmol) were added into Ethanol anhydrous (50 mL) and sonicated for 10 min, and then refluxed at 80 °C for 5h. After washing with pure water in a 1:1 volume ratio, the mixture was filtered and the solvent was evaporated in a dry box at 60 °C to obtain the final product SD. Then, SD mixed with mercury ion solution results in a complexation reaction that opens the amide ring of rhodamine to emit fluorescence to be detected [14]. NMR spectral data for SD are shown below: ^{1}H NMR (600 MHz, DMSO-d6) δ (ppm): 9.89 (s, 1H), 9.17 (s, 1H), 7.92 (d, J = 7.5 Hz, 1H), 7.64 – 7.56 (m, 2H), 7.14 (d, J = 7.6 Hz, 1H), 6.90 (d, J = 3.1 Hz, 1H), 6.83 (dd, J = 8.9, 3.1 Hz, 1H), 6.71 (d, J = 8.9 Hz, 1H), 6.44 – 6.42 (m, 2H), 6.41 (s, 1H), 6.35 (d, J = 2.6 Hz, 1H), 6.34 (d, J = 1.6 Hz, 2H), 3.65 (s, 3H), 3.31 (s, 4H), 3.29 (d, J = 7.2 Hz, 4H), 1.07 (d, J = 6.8 Hz, 12H).

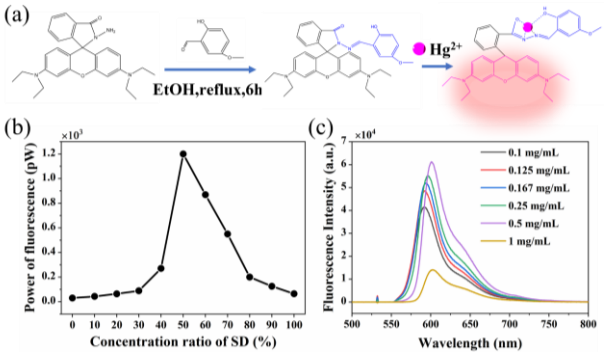

Fig. 3. (a) The synthesis of the SD probe and interaction with Hg^{2+}. (b) Job's plot between SD probes and Hg^{2+}. (c) Fluorescence spectra of different concentrations of SD probes added to the same solution of mercury ions.

To maximize the fluorescence intensity, we optimized the concentration of SD and the volume ratio of SD to mercury ions by Job's plot working curve. Due to the insoluble nature of SD probes, Dimethylformamide (DMF) was chosen as the solvent. In the Job's plot test, the concentration of Hg^{2+} was kept at 20 ng/L and SD at 0.25 mg/L, while changing the volume ratio of SD probes. As illustrated in Fig. 3(b), the highest fluorescence intensity was observed when the volume ratio of the probe SD to Hg^{2+} was 1:1. Based on the aforementioned optimization experiments, a concentration of 0.25 mg/L for the SD probe and the volume ratio of SD to Hg^{2+} of 1:1 was selected for the subsequent experiments on Hg^{2+} concentration and fluorescence intensity.

In optimizing the SD probe concentration, we prepared the SD probes with concentrations of 0.1 mg/L, 0.125 mg/L, 0.167 mg/L, 0.25 mg/L, 0.5 mg/L, and 1 mg/L, while maintaining a fixed concentrate of mercury ion standard solution at 25 ng/L. As depicted in Fig. 3(c), it can be found that the fluorescence intensity was too weak at low concentrations due to incomplete complexation reactions, while the fluorescent spectrum was red-shifted and the fluorescence intensity is reduced at higher concentrations due to the Aggregation-Caused Quenching effects [15]. Therefore, a moderate concentration had to be chosen, here we chose an SD solution of 0.25 mg/mL for subsequent experiments.

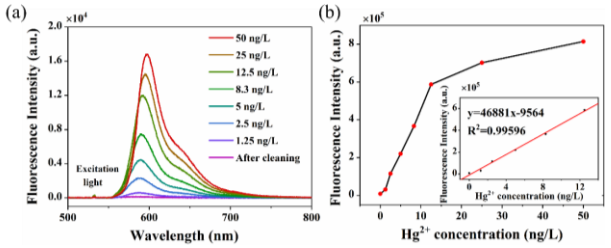

Fig. 4. (a) Fluorescence spectra of the SD solution mixed with different Hg^{2+} concentrations at 532 nm with the optical power of 0.326 mW. (b) Fluorescence intensity changes as a function of Hg^{2+} concentration.

To investigate the relationship between Hg^{2+} concentration and fluorescent intensity, we conducted an Hg^{2+} concentration gradient experiment using a spectrometer. As shown in Fig. 4(a), the fluorescence spectra of different concentrations of Hg^{2+} under the wavelength of 532 nm and power of 0.326 mW exhibited a spectral intensity peak at 590 nm, which is consistent with the fluorescence band of rhodamine-like substances. The figure also reveals a small leakage at 532 nm after the filter, indicating good filtering performance. The light intensity within the 550-700 nm range was integrated to plot the integrated light intensity versus Hg^{2+} concentration. A linear fitted curve has been generated for part of the concentrations, which is shown in Fig. 4(b). The black line represents the integrated fluorescence intensity at different Hg^{2+} concentrations, while the red line represents the linear part of the black line. The results conform well to the linear fitting curves between concentration and fluorescence intensity when Hg^{2+} concentration ranges from 1.25 ng/L to 12.5 ng/L. When the concentration of Hg^{2+} exceeds this range, it can be diluted before detection. Based on the concentration corresponding to three times the standard deviation of the blank control measurement, the limit of detection (LOD) of Hg^{2+} was determined to be 2.3 ng/L [16]. Furthermore, it is worth noting that if the concentrations of Hg^{2+} are too high, the fluorescence spectrum will be red-shifted and the fluorescence intensity will not increase linearly due to the fluorescence quenching phenomenon caused by excessive concentration.

Finally, we conducted a test to evaluate the interference resistance and specificity of the fluorescence probe SD using a photodetector. A mixture of standard solutions of different metal ions (As^{3+}, Fe^{3+}, Cd^{2+}, Ag^{+}, Mn^{2+}, Pb^{2+}, Cu^{2+}, Cr^{2+}, Na^{+}, Hg^{2+}, blank) was prepared at a concentration of 5 μg/L with 0.25 mg/L SD solution in a 1:1 volume ratio and injected into the device. As shown in Fig. 5, the other metal ions produced very weak fluorescence with the SD probe at the same concentration indicating that the SD probe has minimal impact on other particles and specifically targets mercury ions, which demonstrates the high interference resistance and specificity of the SD probe.

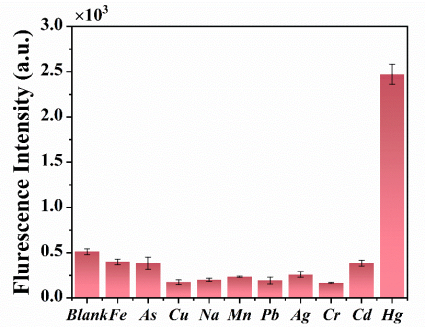

Fig. 5. Fluorescence intensity of different heavy metal ions (As^{3+}, Fe^{3+}, Cd^{2+}, Ag^{+}, Mn^{2+}, Pb^{2+}, Cu^{2+}, Cr^{2+}, Na^{+}, Hg^{2+}, blank) added to the SD probes.

In summary, an all-fiber fluorescence sensing system for online detection and monitoring of mercury ions is reported. In this work, a mercury ion fluorescent probe SD was successfully synthesized and characterized. The developed system demonstrated the fluorescent enhancement effect of the MLHCF and the good optical transmission, achieving an impressive detection limit as low as 2.3 ng/L. Experimentally, we demonstrated the specificity of the SD probe for mercury ions and also found a linear correlation between mercury ion concentration and fluorescence intensity at mercury ion concentrations of 1.25-12.5 ng/L. The comparison of the experimental results with other assays is shown in Table 1. The developed fluorescence detection system demonstrates a detection limit three orders of magnitude lower than that of other fluorescence detection systems.

Table 1. Comparison of fluorescence detection based on MLHCFs with other Hg^{2+} detection methods

Year	Detect method	Probe	LOD	Ref.
2018	Fluorescent	dots-gold nanoclusters	8.7 nM (1.7 μg/L)	[17]
2020	Raman	AuNPs/ITO film	1 ppt (1 ng/L)	[18]
2022	Electrochemical	Graphene Oxide	0.62 nM (124 ng/L)	[19]
2023	Fluorescent	three-dimensional upconversion nanoclusters	0.28 μg/L	[20]
2023	Fluorescent	graphitic carbon nitride nano sheets	27 nM (5.4 μg/L)	[21]
This paper	Fluorescent	rhodamine derivative	2.3 ng/L	

This study used an optical fiber enhancement effect in combination with a fluorescent probe to achieve the detection of low concentrations of Hg^{2+}, providing a new perspective for the detection of trace heavy metal ions in water, which will play an important role in the future of water quality testing. Based on this work, the technique can be combined with heavy metal ion enrichment techniques and other signal enhancement techniques to achieve further enhanced fluorescence signals and lower detection limits [22].

Funding. This work was sponsored by National Natural Science Foundation of China (61875083, 61535005), Social Development Project of Jiangsu Province (BE2019761), the Key Research and Development Program of Shandong Province (2020CXGC011304)

Disclosures. The authors declare no conflicts of interest.

Data availability. Data underlying the results presented in this paper are not publicly available at this time but may be obtained from the authors upon reasonable request.

References

1. L. Jiang, L. Wang, B. Zhang, G. Yin, and R. Y. Wang, European Journal of Inorganic Chemistry, 4438-4443 (2010).
2. M. Berlin, R. K. Zalups, and B. A. Fowler, Handbook on the Toxicology of Metals (Fourth Edition) II, 1013-1075 (2015).
3. H. Huang, Y. Tian, M. D. Zhang, T. R. Xu, D. Mu, P. P. Chen, and W. G. Chu, Spectroscopy and Spectral Analysis 41, 3782-3790 (2021).
4. Y. Gu, G. W. Meng, M. L. Wang, Q. Huang, C. H. Zhu, and Z. L. Huang, Science China-Materials 58, 550-558 (2015).
5. Z. L. Zhu, and Q. Qin, Spectroscopy and Spectral Analysis 28, 1176-1180 (2008).
6. M. Formica, V. Fusi, L. Giorgi, M. Micheloni, Coordination Chemistry Reviews 256.1-2:170-192 (2012).
7. A. Chatterjee, M. Santra, N. Won, S. Kim, J. K. Kim, S. B. Kim, and K. H. Ahn, Journal of the American Chemical Society 131, 2040-+ (2009).
8. T. H. Nguyen, S. P. Wren, T. Sun, and K. T. V. Grattan, in SPIE BioPhotonics Australasia Conference (2016).
9. T. H. Nguyen, T. Sun, and K. T. V. Grattan, Sensors 19 (2019).
10. H. N. Ding, D. J. J. Hu, X. T. Yu, X. X. Liu, Y. F. Zhu, and G. H. Wang, Photonics 9 (2022).
11. B. L. Li, D. R. Li, J. H. Chen, Z. Y. Liu, G. H. Wang, X. P. Zhang, F. Xu, Y. Q. Lu, SENSORS AND ACTUATORS B (2018).
12. H. Cai, X. T. Yu, Q. Chu, Z. Q. Jin, B. Lin, and G. H. Wang, Chinese Optics Letters 17 (2019).
13. Q. Chu, Z. Q. Jin, X. T. Yu, C. X. Li, W. H. Zhang, W. B. Ji, B. Lin, P. P. Shum, X. P. Zhang, and G. H. Wang, Optics Express 27, 10370-10382 (2019).
14. P. Wu, H. Ren, D. Han, W. Gao, and F. Lu, Modern Chemical Industry 40, 238-242 (2020).
15. Y. H. Xu, Y. Zhou, W. H. Ma, S. X. Wang, and S. Y. Li, Journal of Nanoparticle Research 15 (2013).
16. Loock, H. P., Hans Peter, and P. D. Wentzell, Sensors & Actuators B Chemical, 157-163 (2012).
17. W. Liu, X. Wang, Y. Wang, J. Li, D. Shen, Q. Kang, and L. Chen, Sensors and Actuators B: Chemical, 810-817 (2018).
18. X. Guo, F. Chen, F. Wang, Y. Wu, and Q. Ke, Chemical Engineering Journal 390, 124528 (2020).
19. A. Mejri, G. Mandriota, H. Elfil, M. L. Curri, C. Ingrosso, and A. Mars, Molecules 27, 8490 (2022).
20. H. Li, Q. Bei, W. Zhang, M. Marimuthu, M. M. Hassan, S. A. Haruna, and Q. Chen, Food Chemistry 422, 136202 (2023).
21. Y. G. A. El-Reash, E. A. Ghaith, O. El-Awady, F. K. Algethami, H. Lin, E. A. Abdelrahman, and F. S. Awad, Journal of Analytical Science and Technology 14 (2023).
22. Y. Hong, Lama, W. Y. Jacky, and B. Z. Tang, Chemical Communications (2009).

References

1. L. Jiang, L. Wang, B. Zhang, G. Yin, and R. Y. Wang, "Cell Compatible Fluorescent Chemosensor for Hg2+ with High Sensitivity and Selectivity Based on the Rhodamine Fluorophore", European Journal of Inorganic Chemistry, 4438-4443 (2010).
2. M. Berlin, R. K. Zalups, and B. A. Fowler, "Mercury - ScienceDirect", Handbook on the Toxicology of Metals (Fourth Edition) II, 1013-1075 (2015).
3. H. Huang, Y. Tian, M. D. Zhang, T. R. Xu, D. Mu, P. P. Chen, and W. G. Chu, "Design and Batchable Fabrication of High Performance 3D Nanostructure SERS Chips and Their Applications to Trace Mercury Ions Detection", Spectroscopy and Spectral Analysis 41, 3782-3790 (2021).
4. Y. Gu, G. W. Meng, M. L. Wang, Q. Huang, C. H. Zhu, and Z. L. Huang, "R6G/8-AQ co-functionalized Fe3O4@SiO2 nanoparticles for fluorescence detection of trace Hg2+ and Zn2+ in aqueous solution", Science China-Materials 58, 550-558 (2015).
5. Z. L. Zhu, and Q. Qin, "Recent development of speciation analysis for trace arsenic", Spectroscopy and Spectral Analysis 28, 1176-1180 (2008).
6. C. Zhang, and Y. Gao, "Reaction-based fluorescence probe for the detection of metal ions", Chemical Industry and Engineering Progress 35, 3288-3294 (2016).
7. A. Chatterjee, M. Santra, N. Won, S. Kim, J. K. Kim, S. B. Kim, and K. H. Ahn, "Selective Fluorogenic and Chromogenic Probe for Detection of Silver Ions and Silver Nanoparticles in Aqueous Media", Journal of the American Chemical Society 131, 2040-+ (2009).
8. T. H. Nguyen, S. P. Wren, T. Sun, and K. T. V. Grattan, "Fluorescent optical fibre chemosensor for the detection of mercury," in SPIE BioPhotonics Australasia Conference (2016).
9. T. H. Nguyen, T. Sun, and K. T. V. Grattan, "A Turn-On Fluorescence-Based Fibre Optic Sensor for the Detection of Mercury", Sensors 19 (2019).
10. H. N. Ding, D. J. J. Hu, X. T. Yu, X. X. Liu, Y. F. Zhu, and G. H. Wang, "Review on All-Fiber Online Raman Sensor with Hollow Core Microstructured Optical Fiber", Photonics 9 (2022).
11. B. L. Li, D. R. Li, J. H. Chen, Z. Y. Liu, G. H. Wang, X. P. Zhang, F. Xu, Y. Q. Lu, “Hollow core micro-fiber for optical wave guiding and microfluidic manipulation”, SENSORS AND ACTUATORS B (2018).
12. H. Cai, X. T. Yu, Q. Chu, Z. Q. Jin, B. Lin, and G. H. Wang, "Hollow-core fiber-based Raman probe extension kit for in situ and sensitive ultramicro-analysis", Chinese Optics Letters 17 (2019).
13. Q. Chu, Z. Q. Jin, X. T. Yu, C. X. Li, W. H. Zhang, W. B. Ji, B. Lin, P. P. Shum, X. P. Zhang, and G. H. Wang, "Volumetric enhancement of Raman scattering for fast detection based on a silver-lined hollow-core fiber", Optics Express 27, 10370-10382 (2019).
14. P. Wu, H. Ren, D. Han, W. Gao, and F. Lu, "Research progress onoff-onfluorescent probes for Cu(Ⅱ) ion", Modern Chemical Industry 40, 238-242 (2020).
15. Hong Y., Lam J. W. Y., Tang B. Z., “Aggregation-induced emission: phenomenon, mechanism and applications”, Chem. Commun., 4332-4353 (2009).
16. Loock, H. P., Hans Peter, and P. D. Wentzell, “Detection limits of chemical sensors: Applications and misapplications”,Sensors & Actuators B Chemical, 157-163 (2012).
17. W. Liu, X. Wang, Y. Wang, J. Li, D. Shen, Q. Kang, and L. Chen, “Ratiometric fluorescence sensor based on dithiothreitol modified carbon dots-gold nanoclusters for the sensitive detection of mercury ions in water samples”, Sensors and Actuators B: Chemical, 810-817 (2018).
18. X. Guo, F. Chen, F. Wang, Y. Wu, and Q. Ke, “Recyclable Raman Chip for Detection of Trace Mercury Ions”, Chemical Engineering Journal 390, 124528 (2020).
19. A. Mejri, G. Mandriota, H. Elfil, M. L. Curri, C. Ingrosso, and A. Mars, “Electrochemical Sensors Based on Au Nanoparticles Decorated Pyrene-Reduced Graphene Oxide for Hydrazine, 4-Nitrophenol and Hg2+ Detection in Water”, Molecules 27, 8490 (2022).
20. H. Li, Q. Bei, W. Zhang, M. Marimuthu, M. M. Hassan, S. A. Haruna, and Q. Chen, “Ultrasensitive fluorescence sensor for Hg2+ in food based on three-dimensional upconversion nanoclusters and aptamer-modulated thymine-Hg2+-thymine strategy”, Food Chemistry 422, 136202 (2023).
21. Y. G. A. El-Reash, E. A. Ghaith, O. El-Awady, F. K. Algethami, H. Lin, E. A. Abdelrahman, and F. S. Awad, “Highly fluorescent hydroxyl groups functionalized graphitic carbon nitride for ultrasensitive and selective determination of mercury ions in water and fish samples”, Journal of Analytical Science and Technology 14 (2023).
22. Y. H. Xu, Y. Zhou, W. H. Ma, S. X. Wang, and S. Y. Li, "Functionalized magnetic core-shell Fe3O4@SiO2 nanoparticles for sensitive detection and removal of Hg2+", Journal of Nanoparticle Research 15 (2013).